Published in final edited form as:

Biomacromolecules. 2015 March 09; 16(3): 1050–1061. doi:10.1021/acs.biomac.5b00099.

Biomineralized Matrices Dominate Soluble Cues To Direct Osteogenic Differentiation of Human Mesenchymal Stem Cells through Adenosine Signaling

Heemin Kang[†,‡], **Yu-Ru V. Shih**[†], and **Shyni Varghese**[†,‡,*]

[†]Department of Bioengineering, University of California, San Diego, La Jolla, California 92093, United States

[‡]Materials Science and Engineering Program, University of California, San Diego, La Jolla, California 92093, United States

Abstract

Stem cell differentiation is determined by a repertoire of signals from its microenvironment, which includes the extracellular matrix (ECM) and soluble cues. The ability of mesenchymal stem cells (MSCs), a common precursor for the skeletal system, to differentiate into osteoblasts and adipocytes in response to their local cues plays an important role in skeletal tissue regeneration and homeostasis. In this study, we investigated whether a bone-specific calcium phosphate (CaP) mineral environment could induce osteogenic differentiation of human MSCs, while inhibiting their adipogenic differentiation, in the presence of adipogenic-inducing medium. We also examined the mechanism through which the mineralized matrix suppresses adipogenesis of hMSCs to promote their osteogenic differentiation. Our results show that hMSCs cultured on mineralized matrices underwent osteogenic differentiation despite being cultured in the presence of adipogenic medium, which indicates the dominance of matrix-based cues of the mineralized matrix in directing osteogenic commitment of stem cells. Furthermore, the mineralized matrix-driven attenuation of adipogenesis was reversed with the inhibition of A2b adenosine receptor (A2bR), implicating a role of adenosine signaling in mineralized environment-mediated inhibition of adipogenesis. Such synthetic matrices with an intrinsic ability to direct differentiation of multipotent adult stem cells toward a targeted phenotype while inhibiting their differentiation into other lineages not only will be a powerful tool in delineating the role of complex microenvironmental cues on stem cell commitment but also will contribute to functional tissue engineering and their translational applications.

Graphical Abstract

[*]Corresponding Author: svarghese@ucsd.edu; Tel.: +1-858-822-7920; Fax: +1-858-534-5722.

Notes

The authors declare no competing financial interest.

Supporting Information

Figure S1: Adhesion and growth of hMSCs on various matrices under different medium conditions. Table S1: List of primer sequences used in quantitative PCR analyses. This material is available free of charge via the Internet at http://pubs.acs.org.

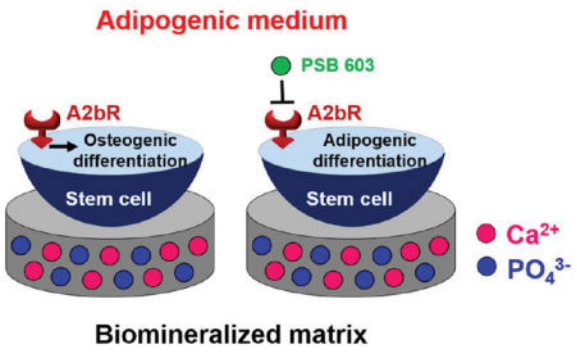

1. INTRODUCTION

Adult stem cells such as mesenchymal stem cells (MSCs) have been shown to differentiate into osteoblasts, adipocytes, and chondrocytes by responding to soluble cues.[1–3] MSCs have been considered to be precursors for osteoblasts and adipocytes, and their ability to differentiate into desirable somatic cell types by responding to tissue-specific requirements is key to maintaining musculoskeletal tissue homeostasis and repair. Maintaining a strict balance between osteogenesis and adipogenesis has been considered to be a prerequisite for sustaining healthy skeletal tissue function. A large number of *in vitro* studies point toward the existence of an inverse correlation between adipogenesis and osteogenesis.[4–6] While most of these studies were performed *in vitro*, it is conceivable that such a correlation could also exist *in vivo*. A disruption in the balance of adipogenesis and osteogenesis is often observed in various pathologies that affect the musculoskeletal system.[7] For instance, studies have shown a close relationship between fat and bone mass, where the high fat mass increases the risk of bone fragility.[8,9] Similarly, excessive accumulation of bone marrow adipocytes along with a decline in bone mineral mass is a characteristic of osteoporosis, obesity, diabetes, anorexia nervosa, and skeletal unloading.[7,10] Preserving such a highly coordinated differentiation of multipotent precursors relies on delicate and intricate interactions between cells and the surrounding microenvironment or niche.

Previous studies have identified various biochemical- and hormone-based signaling underlying various musculoskeletal pathologies.[11–14] Some of these biochemical and hormonal factors have been shown to play a direct role in determining differentiation commitment of MSCs toward osteogenic or adipogenic lineages.[15,16] Besides growth factor- or hormone-based signaling, physical and chemical cues of the extracellular matrix also play an equally important role in tissue homeostasis and regeneration through modulating stem cell commitment.[17] This includes MSCs, as their differentiation into numerous specialized phenotypes can be significantly influenced by various matrix-based cues.[18–22] Given the propensity of MSCs to differentiate into osteoblasts and adipocytes, a number of studies have investigated the role of various matrix cues and geometrical constraints in stimulating differentiation of MSCs using mixed media containing osteogenic- and adipogenic-inducing components.[23–25] However, to our knowledge, there are no precedent studies that have investigated the impact of matrix-based cues on directing stem cell fate in the presence of medium conditions providing an opposing effect.

In this study, we address this question by investigating the effect of calcium phosphate (CaP)-rich mineralized environment on differentiation commitment of hMSCs in the presence of adipogenic-inducing medium. We chose a mineralized environment because CaP minerals are a major constituent of bone ECM and play a key role in bone homeostasis and function.[26,27] Additionally, a large number of studies show the prevalent effect of CaP minerals on osteogenic differentiation of stem and progenitor cells.[28–32] A detailed understanding of the effect of mineral environment on differentiation commitment of hMSCs in the presence of adipogenic-inducing medium might provide novel insights into the role of the mineral environment on maintaining bone and marrow homeostasis and function.

2. MATERIALS AND METHODS

2.1. Synthesis of Hydrogels

Poly(ethylene glycol)-diacrylate (PEGDA; M_n = 6 kDa) and *N*-acryloyl 6-aminocaproic acid (A6ACA) were prepared as described elsewhere.[31] In brief, 1 M A6ACA was dissolved in 1 M NaOH, and 2% (w/v) PEGDA was added to this solution. The precursor solution was mixed with 0.5% (w/v) ammonium persulfate (APS) and 0.15% (v/v) *N*,*N*,*N*′,*N*′-tetramethy-lethylenediamine (TEMED) at 25 °C for 15 min to allow free radical copolymerization and yielded cross-linked hydrogels. The resultant ~1 mm thick hydrogel sheets were allowed to reach equilibrium, swelling in phosphate buffered saline (PBS; pH 7.4) for 48 h with two changes of PBS, and then punched into discs of 1 cm^2 (area) × 1 mm (thickness).

2.2. Mineralization of Hydrogels

The hydrogel discs were mineralized as described elsewhere.[31] Briefly, hydrogel discs were incubated in deionized (DI) water for 6 h and subsequently immersed in modified simulated body fluid (m-SBF; pH 7.4) for 6 h. The main ionic components of m-SBF are 142.0 mM Na^+, 5.0 mM K^+, 1.5 mM Mg^{2+}, 2.5 mM Ca^{2+}, 103.0 mM Cl^-, 10.0 mM HCO_3^-, 1.0 mM HPO_4^{2-}, and 0.5 mM SO_4^{2-}.[33] The hydrogels were briefly rinsed in DI water and soaked in a solution containing 40 mM Ca^{2+} and 24 mM HPO_4^{2-} (pH 5.2) at 25 °C for 45 min while using a rotating shaker (VWR mini-shaker; catalog no. 12620-938) at 200 rpm. The hydrogels were briefly rinsed in DI water and further immersed in m-SBF at 37 °C for 48 h with the daily change of m-SBF. The hydrogels were then equilibrated in PBS for 6 h. The mineralized and nonmineralized PEGDA-*co*-A6ACA hydrogels were sterilized in 70% ethanol (EtOH) for 6 h. The EtOH-treated matrices were washed in PBS for 5 days with three daily changes of PBS prior to cell culture.

2.3. Scanning Electron Microscopy (SEM) and Energy Dispersive Spectroscopy (EDS)

SEM imaging was carried out to examine the morphology of biomineralized matrices. The elemental analysis was conducted by using Oxford energy dispersive spectra (EDS) attachment. EDS was performed to examine the presence of calcium and phosphorus elements in biomineralized matrices as well as to determine their atomic ratio (Ca/P). Samples were prepared and imaged as described elsewhere.[32] In brief, samples were rinsed in DI water for 5 min, flash-frozen using liquid nitrogen, and lyophilized for 24 h. The dried

samples were coated with iridium for 7 s by using sputter coater (Emitech, catalog no. K575X) and then imaged under vacuum using Philips XL30 ESEM.

2.4. Calcium and Phosphate Assays

Calcium and phosphate assays were carried out to determine the Ca^{2+} and PO_4^{3-} content of mineralized matrices as well as the dissolution of CaP minerals from the mineralized matrices. To measure the amount of Ca^{2+} and PO_4^{3-}, samples were briefly rinsed in DI water for 5 min and lyophilized for 16 h, and dry weights were measured. The dried samples were homogenized in 0.5 M HCl and vigorously agitated using a rotating shaker at 25 °C for 3 days. The homogenized samples were used for calcium and phosphate assays. To examine the dissociation of CaP minerals into Ca^{2+} and PO_4^{3-} ions from mineralized matrices, equilibrium-swollen mineralized hydrogels were incubated in 1.5 mL of 50 mM Tris-HCl solution (pH 7.4) at 37 °C for 7 days. Approximately 300 μL of incubation solution was collected and replaced by fresh solution on a daily basis to examine the dissolution of CaP minerals as a function of time. Calcium assay was performed according to manufacturer's protocol (calcium reagent set, Pointe Scientific, catalog no. C7503). In brief, 20 μL of sample solution was mixed with 1 mL of calcium assay reagent. The absorbance of the resultant solution was recorded at 570 nm using a UV/vis spectrophotometer (Beckman Coulter, DU 730). Phosphate assay was carried out according to a method used elsewhere.[34] In brief, phosphate assay reagent was prepared by mixing one part 10 mM ammonium molybdate with two parts acetone and one part H_2SO_4. 125 μL of sample solution and 100 μL of 1 M citric acid were added to 1 mL of the phosphate assay reagent. Absorbance of the resultant solution was recorded at 380 nm using a UV/vis spectrophotometer.

2.5. Cell Culture

The hMSCs (Institute for Regenerative Medicine, Texas A&M University) were maintained in growth medium containing high-glucose DMEM, 10% (v/v) fetal bovine serum (FBS; HyClone), 4 mM L-glutamine, and 50 U/mL penicillin/ streptomycin. The cells were passaged at approximately 70% confluence.

Prior to seeding hMSCs, sterile nonmineralized and mineralized hydrogels as well as cell culture-grade coverslips (CS; diameter = 15 mm, Fisherbrand, catalog no. 1254582) were incubated in growth medium at 37 °C for 24 h to promote cell adhesion. Passage 5 (P5) hMSCs were plated at a density of 12 000 cells/cm^2 and cultured for 14 days using either growth medium or adipogenic medium at 37 °C and 5% CO_2, with medium change every 2 days. Adipogenic medium was prepared by supplementing growth medium with 1 μM dexamethasone (Sigma-Aldrich, catalog no. D2915), 200 μM indomethacin (Sigma-Aldrich, catalog no. I7378), 0.5 μM 3-isobutyl-1-methylxanthine (IBMX; Sigma-Aldrich, catalog no. I5879), and 10 μg/mL of insulin (Sigma-Aldrich, insulin from bovine pancreas, catalog no. I6634). For pharmacological inhibition of A2bR, PSB 603 (Tocris Bioscience, catalog no. 3198) was added into growth medium or adipogenic medium at varying concentrations of 0, 0.5, 10, and 100 nM.

2.6. Cell Tracker Labeling

To visualize the attachment and growth of cells cultured on various matrices (nonmineralized and mineralized matrices as well as coverslips) under different medium conditions (growth medium or adipogenic medium), the cells were labeled with CellTracker fluorescent probes (Life Technologies, catalog no. C34552). Briefly, the cells grown on various matrices were incubated in 20 μM CellTracker fluorescent dyes in DMEM at 37 °C for 30 min and then in growth medium at 37 °C for an additional 30 min. The labeled cells were imaged using a fluorescence microscope (Carl Zeiss, Axio Observer A1).

2.7. Quantitative Polymerase Chain Reaction (qPCR) Analysis

qPCR analysis was carried out to examine differences in gene expression of hMSCs cultured on various matrices under different medium conditions. Cells were collected in 1 mL of TRIzol, and their RNA was isolated using a phenol-chloroform extraction method. For each sample, 1 μg of RNA was reverse-transcribed to cDNA using iScript cDNA synthesis kit (Bio-Rad, catalog no. 170-8891) according to manufacturer's protocol. cDNA solution was mixed with SYBR select master mix (Life Technologies, catalog no. 4472908) and primers for various genes. The resulted solution was subject to qPCR analysis using ABI Prism 7700 sequence detection system (Applied Biosystems). The list of primer sequences is shown in Table S1. Gene expression for various osteogenic (RUNX2, OCN, and BSP) as well as adipogenic (PPAR-γ2, αP2, and LPL) markers was evaluated. The expression for each target gene was normalized to that of corresponding housekeeping gene (GAPDH). The expression level was quantified by $2^{-\Delta\Delta C_T}$ values. To compare gene expression of hMSCs cultured on various matrices under different medium conditions, the expression level was normalized to that of the corresponding cultures on coverslips under identical medium conditions and presented as fold expression. To compare gene expression of hMSCs cultured on mineralized matrices using different medium conditions supplemented with PSB 603, the expression level was normalized to that of cells cultured in the corresponding medium conditions devoid of PSB 603 and presented as fold expression.

2.8. Immunofluorescent Staining

Immunofluorescent staining was performed for osteocalcin, a mature osteoblast-specific marker, and perilipin, a mature adipocyte-specific marker. Cells cultured on various matrices under different medium conditions were fixed in 4% formaldehyde at 25 °C for 10 min. The cells were washed with PBS and blocked by a blocking buffer composed of 3% (w/v) BSA and 0.1% (v/v) Triton X-100 dissolved in PBS at 25 °C for 60 min. The fixed cells were incubated in primary antibodies against osteocalcin (1:100; mouse monoclonal, Santa Cruz Biotechnology, catalog no. sc-74495) or perilipin (1:100; rabbit polyclonal, Santa Cruz Biotechnology, catalog no. 67164) diluted in the blocking buffer at 4 °C for 16 h. The cells were washed with PBS, exposed to secondary antibodies raised against mouse (goat anti-mouse, 1:250, Life Technologies, Alexa Fluor 568) or rabbit (goat anti-rabbit, 1:250, Life Technologies, Alexa Fluor 568) and phalloidin (1:100; Life Technologies, Alexa Fluor 488) diluted in the blocking buffer at 25 °C for 60 min, and washed with PBS. The nuclei of cells were stained using Hoechst 33342 solution (2 μg/mL; Life Technologies, catalog no. H1399) at 25 °C for 7 min and washed with PBS. The samples were mounted onto glass slides and

imaged using a fluorescence microscope (Carl Zeiss, Axio Observer A1). The images were taken at a linear mode, and the same exposure time was used for all samples. The background was uniformly subtracted for all images using ImageJ software, where a rolling ball algorithm with a rolling ball radius of 750 pixels was applied.

2.9. Statistical Analysis

GraphPad Prism 5 was used to perform statistical analyses. Two groups were compared using two-tailed Student's *t*-test. Multiple groups were compared by one-way analysis of variance (ANOVA) with Tukey-Kramer posthoc test. *p*-values measuring less than 0.05 were considered to be statistically significant. Asterisks were assigned to represent different levels of statistical significance.

3. RESULTS

3.1. Synthesis and Characterization of Mineralized Matrices

Synthetic matrices were developed by copolymerizing poly(ethylene glycol)-diacrylate (PEGDA) with *N*-acryloyl 6-aminocaproic acid (A6ACA) moieties as described elsewhere.[35] The PEGDA-*co*-A6ACA hydrogel matrices were biomineralized to incorporate CaP moieties into the matrix,[35] where the presence of pendant side chain terminating with carboxyl groups promoted the binding of Ca^{2+} ions and subsequently led to nucleation of CaP minerals. Gross images of mineralized matrices revealed their opaqueness in contrast to transparent nonmineralized controls (Figure 1a). Scanning electron microscopy (SEM) images of mineralized matrices showed a continuous layer of minerals (Figure 1b). Energy dispersive spectroscopy (EDS) analyses confirmed the presence of calcium and phosphorus elements in mineralized matrices with an atomic ratio (Ca/P) of 1.40 (Figure 1b). As expected, no peaks arising from such elements were observed in nonmineralized matrices. Measurements of the Ca^{2+} and PO_4^{3-} content of mineralized matrices showed that they contain 80.4 ± 1.5 mg of Ca^{2+} and 129.4 ± 3.8 mg of PO_4^{3-} per gram of dry weight of matrices (Figure 1c,d), whereas negligible amounts of such ions were detected in nonmineralized matrices. The CaP minerals of the mineralized matrices dissociated into Ca^{2+} and PO_4^{3-} ions in medium devoid of such ions (Figure 1e,f). Mineralized materials initially showed a rapid release of Ca^{2+} and PO_4^{3-} ions into the surrounding medium of Tris buffer within 1 day of incubation; thereafter, their ionic concentration in the surrounding medium did not vary significantly throughout the experimental time of 7 days.

3.2. Culture Condition-Dependent Osteogenesis or Adipogenesis of hMSCs

We cultured hMSCs on non-mineralized and mineralized matrices and coverslips in either growth medium or adipogenic medium. All of the matrices supported adhesion and spreading of cells with no significant differences both in growth medium and adipogenic medium (Figure S1). Cells under all culture conditions proliferated and reached confluence within 10 days of culture. We next determined the effect of mineralized and nonmineralized matrices on differentiation of hMSCs in both growth and adipogenic medium and compared against those cultured on cell culture-grade coverslips under identical conditions. The cells cultured on mineralized matrices in growth medium exhibited a significant upregulation of various osteogenic markers (RUNX2, OCN, and BSP) compared to those on other matrices

under investigation after 14 days of culture, which is in accordance with previous reports (Figure 2a).[29] Unlike osteogenic markers, adipogenic markers (PPAR-γ2, αP2, and LPL) were undetectable on any of the matrices in growth medium (Figure 2a). Findings from the gene expression profile were further confirmed by immunofluorescent staining for osteocalcin (osteoblast-specific marker) and perilipin (adipocyte-specific marker). The cells cultured on mineralized matrices in growth medium stained positive for osteocalcin (Figure 3a), whereas no positive staining for perilipin was observed on any of the matrices in growth medium (Figure 3b), consistent with the lack of adipogenic gene expression. The cells were also stained for F-actin and Hoechst (for nuclei). The gene expression profile along with immunofluorescent staining suggests that the mineralized matrices possess necessary cues to direct osteogenic differentiation of hMSCs in growth medium.

We next examined the effect of different matrices on hMSC differentiation in adipogenic medium. Specifically, we asked whether the cues from the mineralized matrices would be sufficient to direct osteogenic differentiation of hMSCs when cultured in adipogenic medium. The differentiation pattern of hMSCs on different matrices showed that the cells on nonmineralized matrices and coverslips exhibited a significant upregulation of adipogenic markers, whereas those on mineralized matrices had minimal to no expression of adipogenic markers (Figure 2b). Instead of undergoing adipogenesis, the cells on mineralized matrices underwent osteogenic differentiation and displayed an upregulation of various osteogenic markers despite being incubated in adipogenic medium (Figure 2b). Immunofluorescent staining for osteocalcin and perilipin further corroborated the findings from the gene expression. The hMSCs on mineralized matrices stained positive for osteocalcin (Figure 4a), with minimal to no positive staining for perilipin (Figure 4b). On the contrary, cells on nonmineralized matrices and coverslips stained positive for perilipin (Figure 4b) and exhibited no positive staining for osteocalcin (Figure 4a). Taken together, the results suggest that the cues provided by the mineralized matrices are effectively dominant in directing osteogenic differentiation of hMSCs while inhibiting their adipogenic differentiation, even in the presence of medium conditions that are known to drive adipogenic differentiation of hMSCs.

3.3. Role of Adenosine Signaling in Mineralized Matrix-Mediated Osteogenesis and Inhibition of Adipogenesis

We have previously demonstrated the role of adenosine signaling in mineralized matrix-assisted osteogenesis of hMSCs.[30] Thus, we wondered whether adenosine signaling not only promotes osteogenic differentiation of hMSCs but also attenuates their adipogenic differentiation in a mineral environment. In order to investigate the role of adenosine signaling in inhibition of adipogenesis on mineralized matrices, we examined the role of adenosine A2b receptor (A2bR). We chose A2bR due to its established role in mineralized matrix- mediated osteogenic differentiation of hMSCs.[30] We blocked A2bR with 8-[4-[4-(4-chlorophenzyl)piperazide-1-sulfonyl)-phenyl]]-1-propylxanthine (PSB 603) to examine its effect on mineralized matrix-assisted suppression of adipogenesis of hMSCs. Consistent with our previous report, the hMSCs cultured on mineralized matrices in growth medium showed downregulation of osteogenic markers (RUNX2, OCN, and BSP) in the presence of PSB 603 (Figure 5a).[30] The downregulation of osteogenic markers was further confirmed by

immunofluorescent staining for osteocalcin, which showed that the positive signal of hMSCs on mineralized matrices diminished significantly in the presence of PSB 603 (Figure 6a). The presence of PSB 603 in growth medium did not have any effect on adipogenesis, and the expression levels of various adipogenic markers remained undetectable (Figure 5a). The cells on mineralized matrices stained negative for perilipin, both in the presence and absence of PSB 603 in growth medium (Figure 6b), further confirming no influence of PSB 603 on adipogenic differentiation of hMSCs.

We next investigated the effect of adenosine signaling on mineralized matrix-mediated inhibition of adipogenesis in adipogenic medium. Similar to the cultures in growth medium, the hMSCs on mineralized matrices exhibited downregulation of osteogenic markers (RUNX2, OCN, and BSP) in adipogenic medium supplemented with PSB 603 (Figure 5b). Concomitant with the decrease in osteogenic gene expression pattern, we observed a significant upregulation of adipogenic markers (PPAR-γ2, aP2, and LPL; Figure 5b). This is in stark contrast to hMSCs on mineralized matrices in adipogenic medium without the inhibition of A2bR. The expression levels of adipogenic genes were found to be the highest for cultures containing 100 nM PSB 603. The gene expression pattern was further confirmed by immunofluorescent staining showing that the addition of PSB 603 into adipogenic medium resulted in the attenuation of positive osteocalcin staining in hMSCs on mineralized matrices (Figure 7a). The reduction in osteocalcin signaling was accompanied by positive staining for perilipin, and its intensity increased as the concentration of PSB 603 in the medium increased (Figure 7b).

4. DISCUSSION

Biomaterials recapitulating tissue-specific physical and chemical cues have been considered to be a powerful tool in directing stem cell differentiation commitment. Prevalent use of biomaterials to direct stem cell commitment to assist tissue repair, however, is dependent upon the dominancy of the matrix-based cues over competing soluble cues present in the milieu. This is paramount when the cells possess multipotency and a shift in differentiation of the progenitor cells could lead to pathologies. Biomaterials containing CaP minerals promote osteogenic differentiation of progenitor and stem cells,[28,29,31,32] and a number of studies have used such mineralized materials to promote bone tissue formation *in vivo*.[31,36,37] Given the propensity of MSCs to differentiate into both osteoblasts and adipocytes in response to the matrix or soluble cues, we examined the fate decision of hMSCs in an environment where disparate instructive cues are presented: the mineralized matrix provides cues relevant to osteogenesis, whereas the adipogenic medium provides cues necessary for adipogenesis.

Our results showed that hMSCs cultured on various matrices in the presence and absence of adipogenic soluble supplements underwent differential fate commitment into either osteogenic or adipogenic lineages, depending upon the local cues available from the matrices and/or medium conditions. Specifically, hMSCs on nonmineralized hydrogels and coverslips underwent adipogenic differentiation in adipogenic medium, and no significant differentiation was observed in growth medium. However, intriguingly, hMSCs cultured on mineralized matrices underwent osteogenic differentiation, while inhibiting their adipogenic

differentiation, despite being cultured in adipogenic medium. The inhibition of adipogenesis in the presence of adipogenic medium was observed only on CaP-bearing matrices, indicating that the matrix-mediated inhibition is largely attributed to the mineral environment. A previous study by Jensen et al. reported a similar finding, where the authors observed a significant decline in adipogenic differentiation of 3T3-L1 preadipocytes in adipogenic medium containing high levels of calcium supplements.[38] A number of studies have shown the importance of dissolution of CaP minerals in determining the osteoinductivity of mineralized matrices.[37] Biomineralized matrices used in this study contained apatite-like CaP minerals[35] that can be easily dissociated into Ca^{2+} and $PO4^{3-}$ ions. The dissolution and precipitation of CaP moieties regulate the levels of Ca^{2+} and PO_4^{3-} ions in the extracellular milieu.[37,39,40]

The mineralized matrix-assisted attenuation of adipogenesis of hMSCs was reversed upon blocking of A2bR, a $G\alpha s/\alpha q$ protein-coupled receptor, suggesting the role of adenosine signaling in this process. The adipogenic differentiation of hMSCs in the presence of A2bR inhibitor was accompanied by inhibition of their osteogenic differentiation. This is in accordance with previous reports that have implicated the role of adenosine signaling, in particular, A2bR, on osteogenic differentiation of MSCs[30,41,42] and our previous findings that adenosine signaling through phosphate metabolism and A2bR plays an important role in mineralized matrix-assisted osteogenic differentiation of hMSCs.[30] Studies have shown that, under culture conditions devoid of osteogenic cues, merely overexpressing A2bR in preosteoblasts increased osteoblast gene expression but inhibited their adipogenesis in adipogenic-inducing medium.[43] This suggests that A2bR signaling plays a key role in specifying osteogenic differentiation of progenitor cells *in vitro*. A2bR activates adenylate cyclase and increases intracellular cAMP levels to play an inhibitory role in adipogenesis.[44,45] Findings in a recent study by Eisenstein et al. further demonstrate that A2bR activation inhibits adipogenic differentiation of preadipocytes through the transcription factor Krüppel-like factor 4 (KLF4), which appears to be partially regulated by an increase in cAMP and activation of PKA.[46] However, other studies have shown that KLF4 directly binds CCAAT/enhancer-binding protein β (C/EBPβ) promoter and is required for adipogenesis,[47] whereas ectopic overexpression of KLF4 attenuated osteoblast differentiation and mineralization.[48] In another study, suppression of KLF4 in hMSCs enhanced both osteogenic and adipogenic differentiation.[49] The discrepant role of KLF4 during osteogenic versus adipogenic fate regulation in these studies implies that the downstream molecular machinery of A2bR is dynamic and context-dependent and remains to be elucidated. Nonetheless, A2bR clearly acts as a molecular switch to arbitrate cell fates in a competing environment containing CaP mineral-borne osteogenic cues and soluble adipogenic cues.

5. CONCLUSIONS

In summary, our results showed that the cues provided by the mineralized matrices promote osteogenic commitment of hMSCs as well as suppress their adipogenic differentiation even in the presence of adipogenic-inducing medium. Interestingly, the mineralized matrix-assisted diminution of adipogenic differentiation could be reversed through inhibition of A2bR signaling. To our knowledge, this is the first investigation of stem cell commitment in the presence of competing matrix-based and soluble cues and demonstration for the

dominance of mineralized matrix-based cues over soluble medium components in directing osteogenic commitment of hMSCs. Mineralized matrices that support osteogenic differentiation of progenitor and stem cells while inhibiting their adipogenic differentiation could have a significant impact in bone tissue regeneration. Since perturbed differentiation commitment of MSCs into adipogenic lineage over osteogenesis is implicated in various bone disorders, such instructive matrices with inherent bone tissue-specific cues could act as a technological platform to study various bone disorders and pathologies.

Supplementary Material

Refer to Web version on PubMed Central for supplementary material.

Acknowledgments

The authors gratefully acknowledge financial support from the National Institutes of Health (NIH; grant R01 AR063184-01A1) and California Institute of Regenerative Medicine (CIRM; RN2-00945 and RT2-01889). The hMSCs used in this study were provided by Texas A&M University from the NIH (grant P40RR017447).

References

1. Deans RJ, Moseley AB. Mesenchymal stem cells: biology and potential clinical uses. Exp Hematol. 2000; 28:875–884. [PubMed: 10989188]
2. Hwang NS, Zhang C, Hwang YS, Varghese S. Mesenchymal stem cell differentiation and roles in regenerative medicine. Wiley Interdiscip Rev: Syst Biol Med. 2009; 1:97–106. [PubMed: 20835984]
3. Baksh D, Song L, Tuan R. Adult mesenchymal stem cells: characterization, differentiation, and application in cell and gene therapy. J Cell Mol Med. 2004; 8:301–316. [PubMed: 15491506]
4. Beresford J, Bennett J, Devlin C, Leboy P, Owen M. Evidence for an inverse relationship between the differentiation of adipocytic and osteogenic cells in rat marrow stromal cell cultures. J Cell Sci. 1992; 102:341–351. [PubMed: 1400636]
5. Jaiswal RK, Jaiswal N, Bruder SP, Mbalaviele G, Marshak DR, Pittenger MF. Adult human mesenchymal stem cell differentiation to the osteogenic or adipogenic lineage is regulated by mitogen-activated protein kinase. J Biol Chem. 2000; 275:9645–9652. [PubMed: 10734116]
6. Cheng SL, Shao JS, Charlton-Kachigian N, Loewy AP, Towler DA. MSX2 promotes osteogenesis and suppresses adipogenic differentiation of multipotent mesenchymal progenitors. J Biol Chem. 2003; 278:45969–45977. [PubMed: 12925529]
7. Rosen CJ, Bouxsein ML. Mechanisms of disease: is osteoporosis the obesity of bone? Nat Clin Pract Rheumatol. 2006; 2:35–43. [PubMed: 16932650]
8. Zhao LJ, Jiang H, Papasian CJ, Maulik D, Drees B, Hamilton J, Deng HW. Correlation of obesity and osteoporosis: effect of fat mass on the determination of osteoporosis. J Bone Miner Res. 2008; 23:17–29. [PubMed: 17784844]
9. Schnitzler CM. Bone quality: a determinant for certain risk factors for bone fragility. Calcif Tissue Int. 1993; 53:S27–S31. [PubMed: 8275376]
10. Devlin MJ, Rosen CJ. The bone–fat interface: basic and clinical implications of marrow adiposity. Lancet Diabetes Endocrinol. 2015; 3:141–147. [PubMed: 24731667]
11. Pino AM, Ríos S, Astudillo P, Fernández M, Figueroa P, Seitz G, Rodríguez JP. Concentration of adipogenic and proinflammatory cytokines in the bone marrow supernatant fluid of osteoporotic women. J Bone Miner Res. 2010; 25:492–498. [PubMed: 19653807]
12. Cao JJ. Effects of obesity on bone metabolism. J Orthop Surg Res. 2011; 6:30–36. [PubMed: 21676245]

13. Makki K, Froguel P, Wolowczuk I. Adipose tissue in obesity-related inflammation and insulin resistance: cells, cytokines, and chemokines. ISRN Inflammation. 2013:139239. [PubMed: 24455420]
14. Misra M, Klibanski A. Anorexia nervosa obesity and bone metabolism. Pediatr Endocrinol Rev. 2013; 11:21–33. [PubMed: 24079076]
15. Scheller EL, Song J, Dishowitz MI, Soki FN, Hankenson KD, Krebsbach PH. Leptin functions peripherally to regulate differentiation of mesenchymal progenitor cells. Stem Cells. 2010; 28:1071–1080. [PubMed: 20506495]
16. Xian L, Wu X, Pang L, Lou M, Rosen CJ, Qiu T, Crane J, Frassica F, Zhang L, Rodriguez JP. Matrix IGF-1 maintains bone mass by activation of mTOR in mesenchymal stem cells. Nat Med. 2012; 18:1095–1101. [PubMed: 22729283]
17. Discher DE, Mooney DJ, Zandstra PW. Growth factors, matrices, and forces combine and control stem cells. Science. 2009; 324:1673–1677. [PubMed: 19556500]
18. Engler AJ, Sen S, Sweeney HL, Discher DE. Matrix elasticity directs stem cell lineage specification. Cell. 2006; 126:677–689. [PubMed: 16923388]
19. Young DA, Choi YS, Engler AJ, Christman KL. Stimulation of adipogenesis of adult adipose-derived stem cells using substrates that mimic the stiffness of adipose tissue. Biomaterials. 2013; 34:8581–8588. [PubMed: 23953825]
20. Dalby MJ, Gadegaard N, Tare R, Andar A, Riehle MO, Herzyk P, Wilkinson CD, Oreffo RO. The control of human mesenchymal cell differentiation using nanoscale symmetry and disorder. Nat Mater. 2007; 6:997–1003. [PubMed: 17891143]
21. Ayala R, Zhang C, Yang D, Hwang Y, Aung A, Shroff SS, Arce FT, Lal R, Arya G, Varghese S. Engineering the cell–material interface for controlling stem cell adhesion, migration, and differentiation. Biomaterials. 2011; 32:3700–3711. [PubMed: 21396708]
22. Benoit DS, Schwartz MP, Durney AR, Anseth KS. Small functional groups for controlled differentiation of hydrogel-encapsulated human mesenchymal stem cells. Nat Mater. 2008; 7:816–823. [PubMed: 18724374]
23. McBeath R, Pirone DM, Nelson CM, Bhadriraju K, Chen CS. Cell shape, cytoskeletal tension, and RhoA regulate stem cell lineage commitment. Dev Cell. 2004; 6:483–495. [PubMed: 15068789]
24. Kilian KA, Bugarija B, Lahn BT, Mrksich M. Geometric cues for directing the differentiation of mesenchymal stem cells. Proc Natl Acad Sci US A. 2010; 107:4872–4877.
25. Guvendiren M, Burdick JA. The control of stem cell morphology and differentiation by hydrogel surface wrinkles. Biomaterials. 2010; 31:6511–6518. [PubMed: 20541257]
26. Bouillon R, Suda T. Vitamin D: calcium and bone homeostasis during evolution. BoneKEy Rep. 2014; 3
27. Barrère F, van Blitterswijk CA, de Groot K. Bone regeneration: molecular and cellular interactions with calcium phosphate ceramics. Int J Nanomed. 2006; 1:317.
28. Müller P, Bulnheim U, Diener A, Lüthen F, Teller M, Klinkenberg ED, Neumann HG, Nebe B, Liebold A, Steinhoff G. Calcium phosphate surfaces promote osteogenic differentiation of mesenchymal stem cells. J Cell Mol Med. 2008; 12:281–291. [PubMed: 18366455]
29. Phadke A, Shih YRV, Varghese S. Mineralized synthetic matrices as an instructive microenvironment for osteogenic differentiation of human mesenchymal stem cells. Macromol Biosci. 2012; 12:1022–1032. [PubMed: 22760917]
30. Shih YRV, Hwang Y, Phadke A, Kang H, Hwang NS, Caro EJ, Nguyen S, Siu M, Theodorakis EA, Gianneschi NC. Calcium phosphate-bearing matrices induce osteogenic differentiation of stem cells through adenosine signaling. Proc Natl Acad Sci US A. 2014; 111:990–995.
31. Kang H, Wen C, Hwang Y, Shih YRV, Kar M, Seo SW, Varghese S. Biomineralized matrix-asssisted osteogenic differentiation of human embryonic stem cells. J Mater Chem B. 2014; 2:5676–5688. [PubMed: 25114796]
32. Kang H, Shih YRV, Hwang Y, Wen C, Rao V, Seo T, Varghese S. Mineralized gelatin methacrylate-based matrices induce osteogenic differentiation of human induced pluripotent stem cells. Acta Biomater. 2014; 10:4961–4970. [PubMed: 25153779]
33. Oyane A, Kim HM, Furuya T, Kokubo T, Miyazaki T, Nakamura T. Preparation and assessment of revised simulated body fluids. J Biomed Mater Res, Part A. 2003; 65:188–195.

34. Heinonen JK, Lahti RJ. A new and convenient colorimetric determination of inorganic orthophosphate and its application to the assay of inorganic pyrophosphatase. Anal Biochem. 1981; 113:313–317. [PubMed: 6116463]
35. Phadke A, Zhang C, Hwang Y, Vecchio K, Varghese S. Templated mineralization of synthetic hydrogels for bone-like composite materials: role of matrix hydrophobicity. Biomacromolecules. 2010; 11:2060–2068. [PubMed: 20690714]
36. Phadke A, Hwang Y, Hee Kim S, Hyun Kim S, Yamaguchi T, Masuda K, Varghese S. Effect of scaffold microarchitecture on osteogenic differentiation of human mesenchymal stem cells. Eur Cells Mater. 2013; 25:114–29.
37. LeGeros RZ. Calcium phosphate-based osteoinductive materials. Chem Rev. 2008; 108:4742–4753. [PubMed: 19006399]
38. Jensen B, Farach-Carson MC, Kenaley E, Akanbi KA. High extracellular calcium attenuates adipogenesis in 3T3-L1 preadipocytes. Exp Cell Res. 2004; 301:280–292. [PubMed: 15530863]
39. Ducheyne P, Radin S, King L. The effect of calcium phosphate ceramic composition and structure on in vitro behavior. I. Dissolution. J Biomed Mater Res. 1993; 27:25–34. [PubMed: 8380596]
40. Radin S, Ducheyne P. The effect of calcium phosphate ceramic composition and structure on in vitro behavior. II. Precipitation. J Biomed Mater Res. 1993; 27:35–45. [PubMed: 8380597]
41. Carroll SH, Wigner NA, Kulkarni N, Johnston-Cox H, Gerstenfeld LC, Ravid K. A2B adenosine receptor promotes mesenchymal stem cell differentiation to osteoblasts and bone formation in vivo. J Biol Chem. 2012; 287:15718–15727. [PubMed: 22403399]
42. Gharibi B, Abraham AA, Ham J, Evans BA. Adenosine receptor subtype expression and activation influence the differentiation of mesenchymal stem cells to osteoblasts and adipocytes. J Bone Miner Res. 2011; 26:2112–2124. [PubMed: 21590734]
43. Gharibi B, Abraham A, Ham J, Evans B. Contrasting effects of A1 and A2b adenosine receptors on adipogenesis. Int J Obes. 2011; 36:397–406.
44. Zhang L, Paddon C, Lewis MD, Grennan-Jones F, Ludgate M. Gsα signalling suppresses PPARγ2 generation and inhibits 3T3L1 adipogenesis. J Endocrinol. 2009; 202:207–215. [PubMed: 19460852]
45. Liu X, Malbon CC, Wang H-y. Identification of amino acid residues of Gsα critical to repression of adipogenesis. J Biol Chem. 1998; 273:11685–11694. [PubMed: 9565589]
46. Eisenstein A, Carroll SH, Johnston-Cox H, Farb M, Gokce N, Ravid K. An adenosine receptor–Krüppel-like factor 4 protein axis inhibits adipogenesis. J Biol Chem. 2014; 289:21071–21081. [PubMed: 24928509]
47. Birsoy K, Chen Z, Friedman J. Transcriptional regulation of adipogenesis by KLF4. Cell Metab. 2008; 7:339–347. [PubMed: 18396140]
48. Kim JH, Kim K, Youn BU, Lee J, Kim I, Shin HI, Akiyama H, Choi Y, Kim N. Kruppel-like factor 4 attenuates osteoblast formation, function, and cross talk with osteoclasts. J Cell Biol. 2014; 204:1063–1074. [PubMed: 24616223]
49. Li J, Dong J, Zhang Zh, Zhang DC, You XY, Zhong Y, Chen MS, Liu SM. miR-10a restores human mesenchymal stem cell differentiation by repressing KLF4. J Cell Physiol. 2013; 228:2324–2336. [PubMed: 23696417]

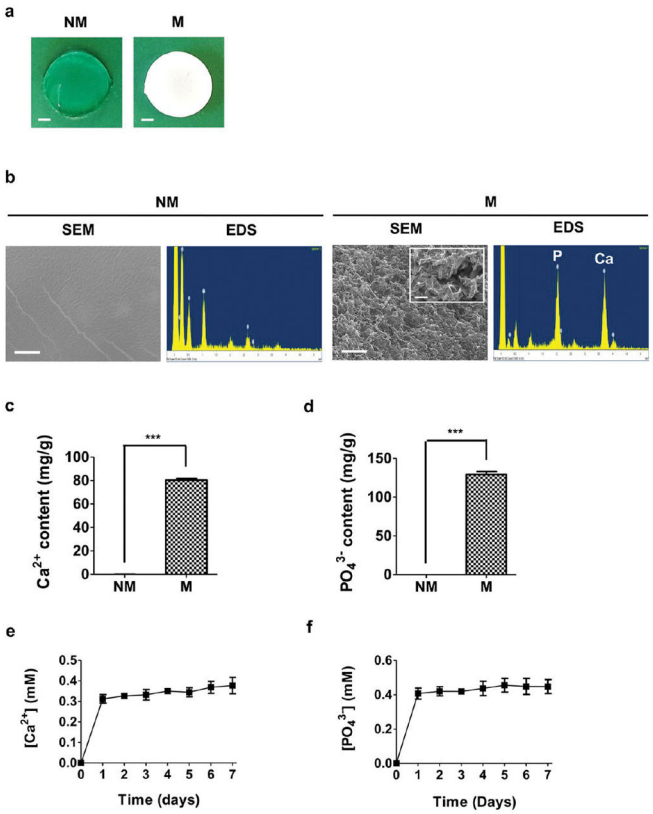

Figure 1.

Characterization of biomineralized matrices. (a) Gross images of nonmineralized (NM) and mineralized (M) hydrogel discs. Scale bars represent 2 mm. (b) Scanning electron microscopy (SEM) images and corresponding energy dispersive spectra (EDS) of nonmineralized and mineralized matrices. Scale bars indicate 2 μm. Inset shows high-magnification images, and scale bar represents 500 nm. (c) Ca^{2+} and (d) PO_4^{3-} amounts of nonmineralized and mineralized matrices after normalization to the dry weight of matrices. Release of (e) Ca^{2+} and (f) $PO4^{3-}$ from mineralized matrices in Tris buffer lacking such ions at 37 °C as a function of time. Data are presented as the mean ± standard deviation ($n = 3$). Two groups were compared by employing two-tailed Student's t-test. Asterisks were assigned to p-values with statistical significance (***, $p < 0.001$).

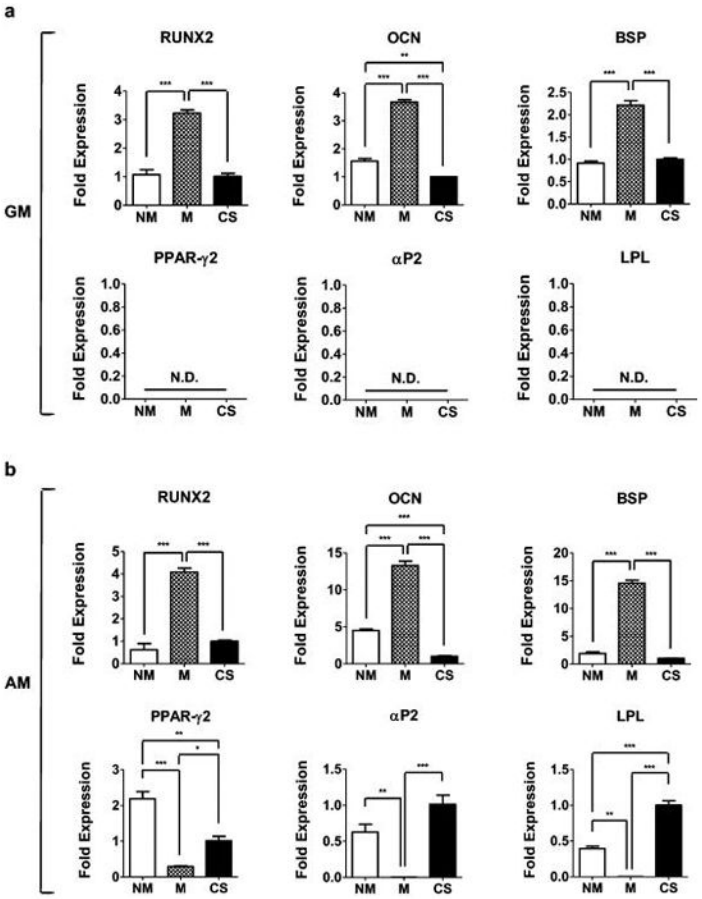

Figure 2.

Quantitative PCR analyses of hMSCs cultured on various matrices under different medium conditions. Gene expressions of hMSCs for osteogenic markers (RUNX2, OCN, and BSP) as well as adipogenic markers (PPAR-γ2, αP2, and LPL) after 14 days of culture. Cells were cultured on nonmineralized (NM) and mineralized (M) matrices and coverslips (CS) in (a) growth medium (GM) and (b) adipogenic medium (AM). N.D. indicates a nondetectable amplification signal. Data are presented as the mean ± standard error ($n = 3$). Groups with different matrices in the same medium were compared by using one-way ANOVA with a Tukey-Kramer posthoc test. Asterisks were assigned to p-values with statistical significance (*, $p < 0.05$; **, $p < 0.01$; ***, $p < 0.001$).

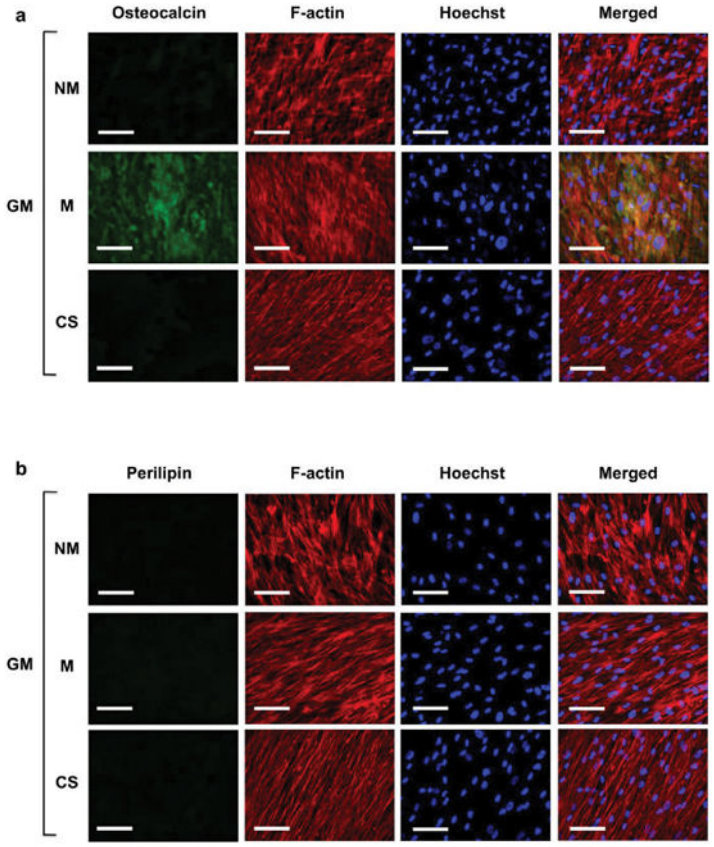

Figure 3.

Immunofluorescent staining of (a) osteocalcin (green) and (b) perilipin (green) with corresponding F-actin (red) and nuclei (blue; Hoechst) for hMSCs on nonmineralized (NM) and mineralized (M) matrices and coverslips (CS) in growth medium (GM) after 14 days of culture. Scale bars represent 100 μm.

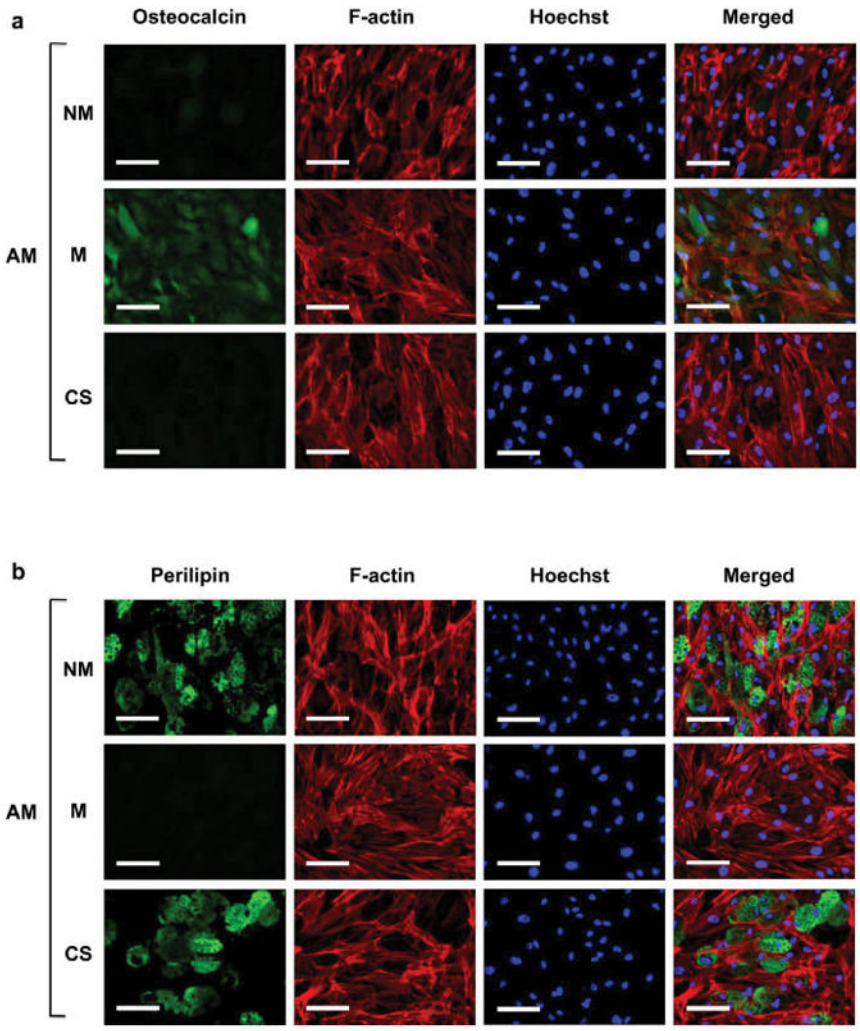

Figure 4.

Immunofluorescent staining of (a) osteocalcin (green) and (b) perilipin (green) with corresponding F-actin (red) and nuclei (blue; Hoechst) for hMSCs on nonmineralized (NM) and mineralized (M) matrices and coverslips (CS) in adipogenic medium (AM) after 14 days of culture. Scale bars represent 100 μm.

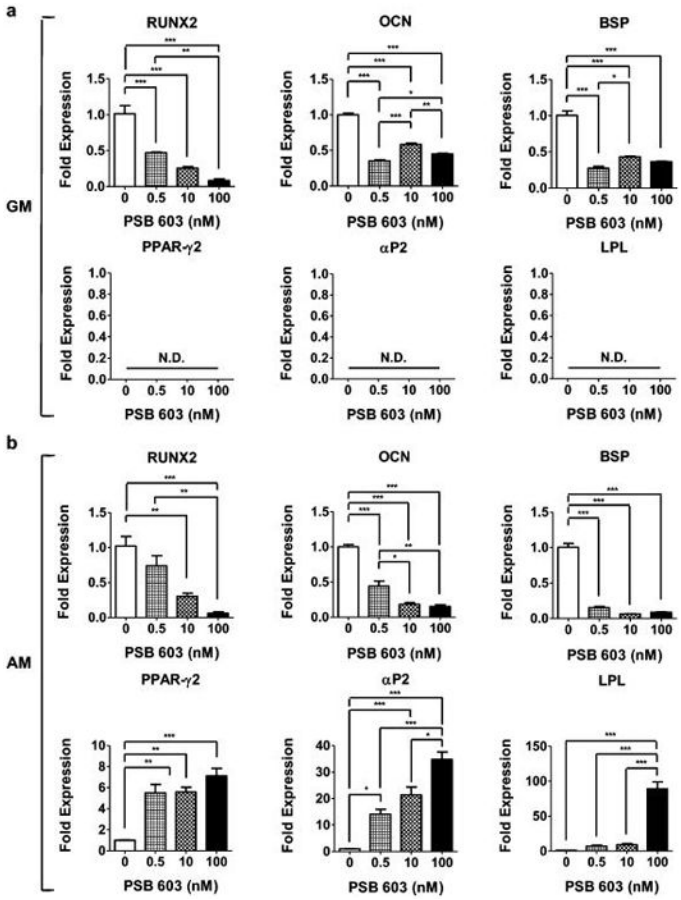

Figure 5.

Quantitative PCR analyses of hMSCs cultured on mineralized matrices under different medium conditions with varying amounts of A2bR antagonist, PSB 603. Fold expressions of hMSCs for osteogenic markers (RUNX2, OCN, and BSP) as well as adipogenic markers (PPAR-γ2, αP2, and LPL) after 14 days of culture. Cells were cultured in (a) growth medium (GM) and (b) adipogenic medium (AM) supplemented with PSB 603 at varying concentrations of 0, 0.5, 10, and 100 nM. N.D. indicates a nondetectable signal from PCR cycles. Data are presented as the mean ± standard error (n = 3). Groups with varying concentrations of PSB 603 under the same medium conditions were compared by using one-way ANOVA with a Tukey-Kramer posthoc test. Asterisks were assigned to p-values with statistical significance (*, $p < 0.05$; **, $p < 0.01$; ***, $p < 0.001$).

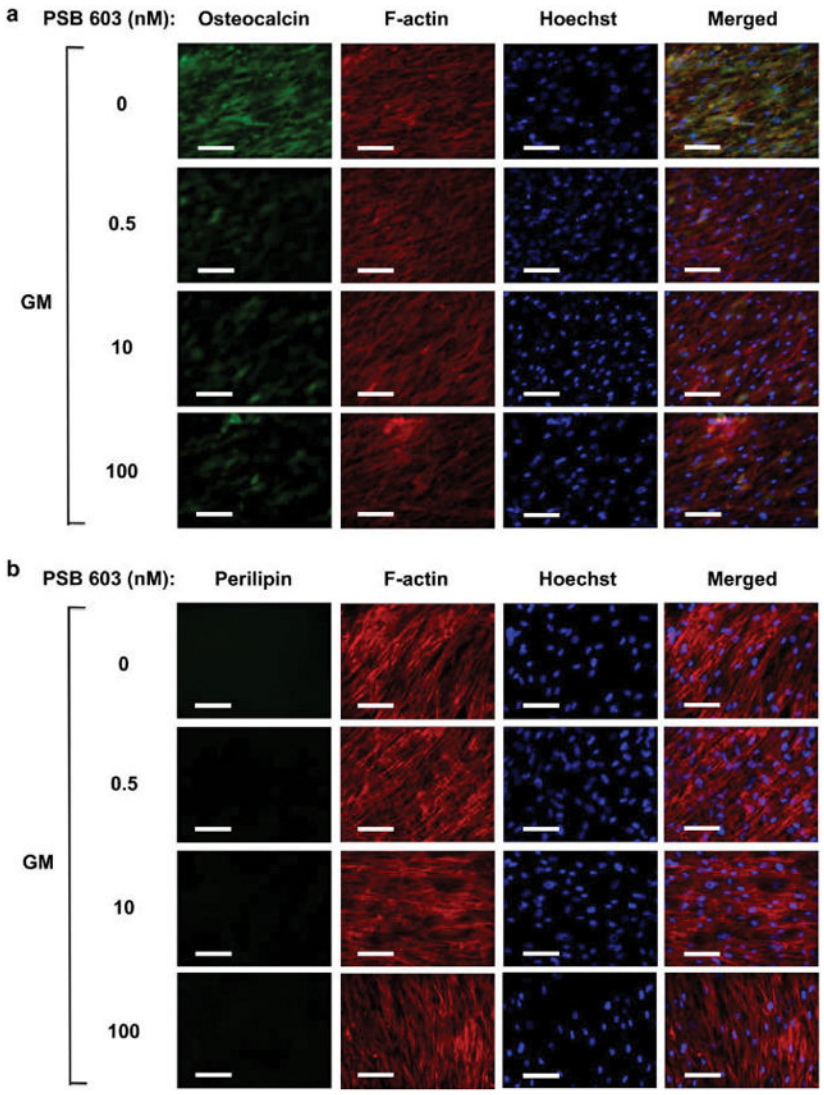

Figure 6.

Immunofluorescent staining of (a) osteocalcin (green) and (b) perilipin (green) with corresponding F-actin (red) and nuclei (blue; Hoechst) for hMSCs on mineralized matrices after 14 days of culture in growth medium (GM) containing varying amounts (0, 0.5, 10, and 100 nM) of an A2bR antagonist, PSB 603. Scale bars represent 100 μm.

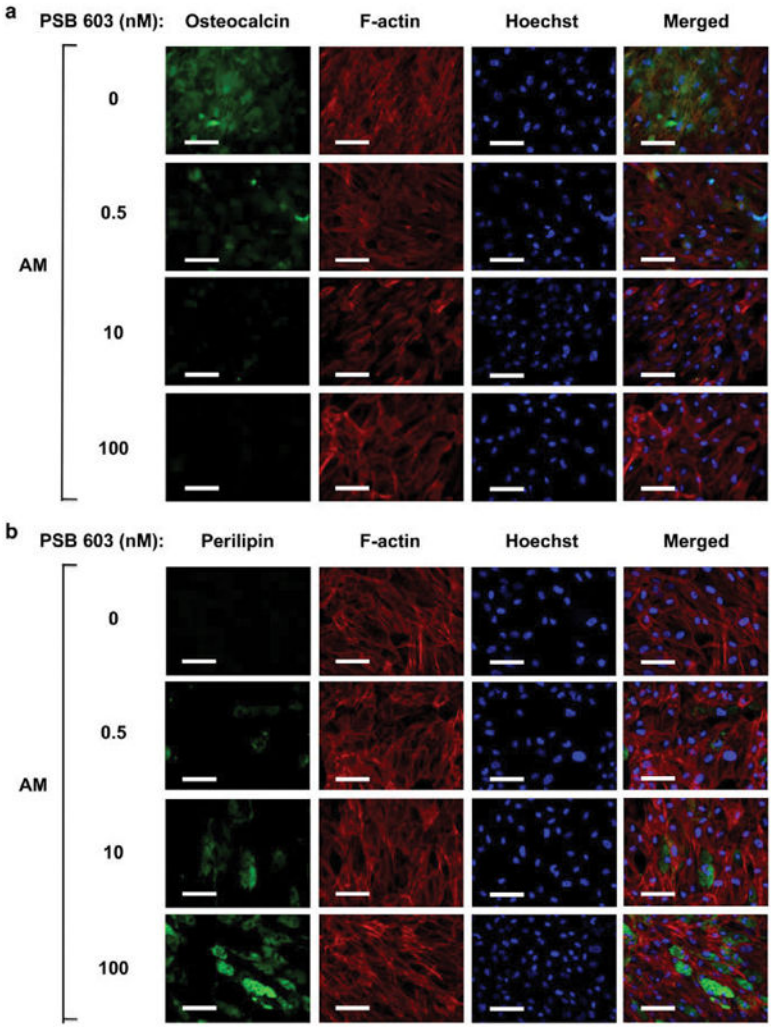

Figure 7.

Immunofluorescent staining of (a) osteocalcin (green) and (b) perilipin (green) with corresponding F-actin (red) and nuclei (blue; Hoechst) for hMSCs on mineralized matrices after 14 days of culture in adipogenic medium (AM) containing varying amounts (0, 0.5, 10, and 100 nM) of an A2bR antagonist, PSB 603. Scale bars represent 100 μm.